ON THE SPATIAL VARIATION OF THE VERTICAL THERMAL DIFFUSION COEFFICIENT IN A SIMPLE OCEAN MODEL

By P.F. Hodnett* and R. McNamara
Department of Mathematics and Statistics, University of Limerick

[Received 16 April 2002. Read 12 September 2002. Published 31 December 2003.]

Abstract

Numerical experiments were conducted on a simple model of the North Atlantic ocean consisting of a thermocline region above an abyssal region with the surface mixing (Ekman) layer excluded. The western ocean boundary (in both the thermocline and abyss) layers are also excluded. It is also assumed that zonal variations in temperature can be neglected. The model temperature field is required to agree with the observed ocean temperature field as given in the Levitus' climatological atlas of the world ocean. This requirement results in a spatial variation for the vertical thermal diffusion coefficient over the combined thermocline/abyss, with values for this coefficient of: $1.35 \times 10^{-4}\text{m}^2\ \text{s}^{-1}$ in the tropical thermocline; $0.675 \times 10^{-4}\text{m}^2\ \text{s}^{-1}$ in the combined subpolar/subtropical thermocline; and a range of $1.49–1.69 \times 10^{-4}\text{m}^2\ \text{s}^{-1}$ in the abyss. These values are similar in magnitude to previous calculations, and result from the assumption that the typical upwelling velocity from the abyss into the thermocline is of order $2 \times 10^{-7}\text{m}^2\ \text{s}^{-1}$. Webb and Suginohara suggest that some abyssal mass rises along isothermals in the southern ocean, with the resultant need for a decrease in diathermal upwelling over the remainder of the global ocean. This implies a smaller value for the typical abyssal upwelling velocity, and if it is reduced by a factor of 5 from the above value, then the resulting values for the vertical thermal diffusion coefficient are close to $3 \times 10^{-5}\text{m}^2\ \text{s}^{-1}$ (representing the average over the whole ocean). Webb and Suginohara suggest that this is more consistent with existing ocean measurements.

1. Introduction

The distribution of heat, salt and tracer substances in the ocean depend on mixing along and across surfaces of equal density (isopycnal and diapycnal mixing, respectively). Here, where saline effects are neglected and it is assumed that density varies only with temperature, the distribution of heat depends on convection of heat by the fluid along isothermal surfaces and diffusion of heat across isothermal surfaces. A measure of the latter effect is given by the value of the coefficient of vertical thermal diffusion, k_z'. Previous theoretical calculations by Munk in [11] found that a value, for k_z' of $10^{-4}\text{m}^2\ \text{s}^{-1}$ was required to support the ocean thermal circulation. However, recent tracer release experiments in the open ocean (distant from ocean boundaries) [9] give values of k_z' near $10^{-5}\text{m}^2\ \text{s}^{-1}$, an order of magnitude lower. In contrast, Polzin *et al*. [15] found much larger values for k_z' (reaching $10^{-3}\text{m}^2\ \text{s}^{-1}$) in localised regions near the rough bottom topography of the mid-Atlantic ridge. More recent theoretical calculations by Munk and Wunsch [12] confirm that the spatially averaged k_z' has a magnitude in the order of $10^{-4}\text{m}^2\ \text{s}^{-1}$.

---

*Corresponding author, e-mail: frank.hodnett@ul.ie

In [24] Webb and Suginohara suggest that some of the abyssal mass rises along isopycnals (here isothermals) in the southern ocean, and should not be included in the diapycnal upwelling from the abyss over the global ocean. With the resulting lowered value of the diapycnal upwelling from the abyss, Webb and Suginohara [24] calculate a revised value for k_z' (averaged over the whole ocean) of $3 \times 10^{-5}\mathrm{m}^2\,\mathrm{s}^{-1}$. There is therefore a lack of agreement as to what is the correct order of magnitude for k_z' (when averaged over the whole ocean). Here we contribute to the current dialogue on this issue for the North Atlantic with a simple ocean model. We require that the model temperature field should agree (as closely as possible) with the observed ocean temperature field as given in the Levitus' climatological atlas of the world ocean [10]. This requirement yields a spatial variation for the vertical thermal diffusion coefficient whose average ocean value is close to $10^{-4}\mathrm{m}^2\,\mathrm{s}^{-1}$ as advocated in [11; 12]. However, if both the upwelling from the abyss and the net upwelling from the thermocline into the Ekman layer are appropriately reduced (as advocated in [24]), then an average ocean value for k_z' near the Webb and Suginohara value in [24] results.

The model considers the ocean to consist of a thermocline region above an abyssal region below the (excluded) surface mixing (Ekman) layer and outside the ocean western boundary layers (in both the thermocline and the abyss). The model for the abyssal region is a modification of the Stommel–Arons abyssal solution in [22; 23], where (for the North Atlantic) a southward flowing western boundary current whose source is a down welling point at the northern extremity of the basin feeds fluid into the abyss. Some of this fluid upwells through the top of abyss into the thermocline and the remainder recirculates in the abyssal region in an anti-cyclonic gyre that closes at the northern extremity source point (with zonal velocity vanishing at the eastern boundary). The thermocline is driven at its base by upwelling through the top of the abyss and a prescribed temperature distribution at the top of the abyss. At the top of the thermocline the distribution of vertical velocity (resulting from the effect of surface wind stress transmitted through the Ekman layer) is prescribed together with the distribution of temperature. In addition it is assumed that the zonal variation of temperature is negligible in comparison to meridional and vertical variations in temperature. Although, as noted in [25], such regions exist in regions of the large oceans (for example the northern Pacific Ocean), over the full extent of the ocean zonal variations of temperature are not negligible. However, the assumption leads to a simplified structure for the velocity field resulting in a linearised equation for temperature so that direct focus on the spatial variation of k_z' is possible in a relatively accessible model. Simple linear models of the ocean have previously been shown to be useful tools through which to clarify aspects of ocean circulation theory [3; 16], and other special solutions of reduced models of the ocean were used in a similar fashion in [17; 18]. The present paper (where the equation describing the temperature is reduced to a linear equation in two dimensions that is readily solved numerically) is offered in the same pedagogical spirit as those papers quoted above.

2. Model

The North Atlantic ocean (between the equator and 60° N) is modelled (with the surface Ekman layer, taken to be 150m deep, excluded) by a thermocline region (150–1500m in depth) over an abyssal region (1500–4200m in depth). However, the influence of the

Ekman layer in the thermocline is retained through prescribing the vertical velocity at the top of the thermocline. This is the effect of the surface wind stress transmitted through the Ekman layer to the top of the thermocline. The ocean (bounded by longitude lines) is taken to be 50° wide. The western ocean boundary layers (in the thermocline and abyss) are not resolved here but are assumed to either supply or receive fluid (from the ocean interior) in conservation of mass. At the eastern boundary a *generalized eastern boundary condition* (to use the terminology of Huang in [6]), of the form $\int u\,dz = 0$ is imposed, where u is the zonal velocity component and the integration is over the total ocean depth. This condition implies that fluid entering the eastern boundary at one depth re-emerges, flowing westward, at another depth (but at the same latitude). This condition, whereby the mass transport at the eastern boundary is zero, has also been used in [8; 13] in modelling the ocean thermocline. The model also assumes that temperature (or, equivalently, density) varies mainly with depth and latitude, and that by comparison its variation with longitude is negligible.

The equations that describe steady motion (below the surface Ekman layer and outside the western boundary layers) in the thermocline and abyss regions are the planetary geostrophic equations, which in non-dimensional form are as follows:

$$\frac{\partial p}{\partial z} = T, \quad 2u\sin\phi = \frac{-\partial p}{\partial \phi}, \quad 2v\sin\phi = \frac{1}{\cos\phi}\frac{\partial p}{\partial \lambda}, \tag{2.1a,b,c}$$

$$\frac{\partial w}{\partial z} = v/\tan\phi, \tag{2.2}$$

$$w\frac{\partial T}{\partial z} + v\frac{\partial T}{\partial \phi} = k\frac{\partial^2 T}{\partial z^2}, \tag{2.3}$$

where (2.2) is the planetary divergence relation that results from the substitution of expressions (2.1b,c) for u and v into the continuity equation. In the above equations λ is longitude (positive eastwards), ϕ is latitude (positive northwards), z is vertical distance (positive upwards), p is pressure, T is temperature, and u, v, w are the respective velocity components in the directions λ, ϕ, z increasing. In Equation (2.3) it is assumed that T is independent of λ and that meridional heat diffusion is negligible in comparison to vertical heat diffusion. It was found through numerical experimentation that when meridional heat diffusion is included at the same order as vertical heat diffusion in the non-dimensional Equation (2.3), then its influence on the solution is negligible, and thus, on the basis of using the simplest possible model, it is set at zero here. For reference the physical variables, denoted by primes ($'$), are given as follows: $(u', v') = U(u, v)$, $w' = Ww$, $z' = Dz$, k'_z (vertical coefficient of heat diffusion) $= DWk$ and temperature t', is given by $T = (t' - t'_0)/t'_0$, where t'_0, taken to be the temperature at the ocean bottom (i.e. at 4200m depth) is 2.0°C. For W we take a typical downwelling vertical velocity from the Ekman layer into the subtropical thermocline, i.e. $W = 10^{-6}\,\text{m s}^{-1}$. In the derivation of the above form for the hydrostatic equation it is assumed that the physical density, ρ', varies only with temperature in the form $\rho' = \rho'_0[1 - \alpha(t' - t'_0)]$, where ρ'_0 is the reference density (taken to be $10^3\,\text{kg m}^{-3}$) and α is the coefficient of thermal expansion (taken to be $2\times10^{-4}(^\circ\text{C})^{-1}$). The pressure p' is written as $p' = -\rho'_0 g z' + \bar{p}$, where g is gravity (taken to be $9.81\,\text{m s}^{-2}$) and $\bar{p} = (\rho'_0 a\Omega U)p$ (where a is the earth's radius taken to be $6.3\times10^6\,\text{m}$ and Ω is the earth's rotation rate taken to be $0.7 \times 10^{-4}\ \mathrm{s}^{-1}$). We also have taken $(g\alpha t_0' D)/(a\Omega u) = 1$ and $U = aW/D$ so that the scale depth, D, and the magnitude, U, of the horizontal speed are given by

$$D = \left[\frac{a^2 \Omega W}{g\alpha t_0'}\right]^{\frac{1}{2}} = 841\mathrm{m} \quad \text{and} \quad U = \left[\frac{W g\alpha t_0'}{\Omega}\right]^{\frac{1}{2}} = 7.49 \times 10^{-3}\mathrm{m\,s}^{-1}. \tag{2.4}$$

Note that $z = 0$ denotes the top of the thermocline, i.e. at depth 150m (thickness of the Ekman layer) below the ocean surface, and that the bottom of the thermocline (at depth 1500m) is at $z = -\gamma$, where $D\gamma = 1350$m, i.e. $\gamma = -1.605$ and the bottom of the abyss (at depth 4200m) is at $z = -3\gamma$.

We take a typical upwelling velocity from the abyss into the thermocline to be $W_a = 2 \times 10^{-7}\mathrm{m\,s}^{-1}$, based on the following considerations. In [21] Stommel took $W_a = 3 \times 10^{-7}\mathrm{m\,s}^{-1}$, and later, in [22; 23], Stommel and Arons suggested that this value is probably too large by a factor of two. An estimate from Yuan *et al*. [26] gives $W_a = 2.25 \times 10^{-7}\mathrm{m\,s}^{-1}$. In his two-level model for the wind and buoyancy forced circulation Huang [7] derives the upwelling velocity at the top of the abyss (these results were later used in [1]), which varies from $5 \times 10^{-6}\mathrm{m\,s}^{-1}$ at the equator to $0.1 \times 10^{-7}\mathrm{m\,s}^{-1}$ at 50° N. His mid-basin values are of order $2 \times 10^{-7}\mathrm{m\,s}^{-1}$. Note that this abyssal upwelling velocity ($W_a = 2 \times 10^{-7}\mathrm{m\,s}^{-1}$) is approximately an order of magnitude smaller than the Ekman downwelling velocity ($W = 10^{-6}\mathrm{m\,s}^{-1}$), which is consistent with what observations suggest.

3. The abyssal region

The solutions for the abyss and thermocline can be determined independently since we have specified *a priori* the position of their common interface (i.e. at depth 1500m), while the temperature distribution (at the interface) is specified from the climatological data given in [10] and the upwelling velocity at the interface between the abyss and thermocline is specified, as above, and is consistent with observations as far as they are known (if the arguments of [21–23] are accepted). Recently, in [24], Webb and Suginohara suggested that some of the abyssal mass rises along isothermals in the southern ocean with the resultant need for a decrease in the diathermal upwelling over the remainder of the global ocean. This would imply a smaller value for the abyssal upwelling velocity than is used here. We will return to this issue again later in the paper. We begin with the abyss since the solution there is easiest to calculate.

3.1. Boundary conditions for abyss

As indicated above:

(i) there is an assigned temperature distribution and upwelling velocity at the top of the abyss, i.e.

$$T = T_a(\phi) \quad \text{and} \quad w = (W_a/W)w_a(\phi) = (0.2)w_a(\phi) \quad \text{at} \quad z = -\gamma, \tag{3.1.1}$$

where the physical vertical velocity at the interface, i.e. $w_a'(\phi)$ is given by

$$w_a'(\phi) = W_a w_a(\phi);$$

(ii) temperature is constant and the normal component of velocity is zero at the (flat) ocean floor, i.e.

$$T=0 \quad \text{and} \quad w=0 \quad \text{at} \quad z=-3\gamma. \tag{3.1.2}$$

An alternative to condition (3.1.2) for the temperature would be to set the vertical heat flux to zero at the bottom of the abyss. Like Pedlosky in [14], we assume constant temperature at the bottom of the abyss. At the eastern boundary the integrated mass transport (from bottom to top of the abyss) is set at zero, i.e. we use a *generalised eastern boundary condition* of the form

$$\int_{z=-3\gamma}^{z=-\gamma} u\,dz=0 \quad \text{at} \quad \lambda=\lambda_E, \tag{3.1.3}$$

where $\lambda=\lambda_E$ (a line of longitude) is the eastern boundary of the North Atlantic with $\lambda_E=5\pi/18$.

3.2. Solution for the abyss

When T is assumed to be independent of λ then Equations (2.1a) and (2.1c) imply that v is independent of z, so that (2.2) can be integrated to give (with boundary conditions (3.1.1) and (3.1.2)):

$$w=(0.1)w_a(\phi)(3+z/\gamma), \quad v=(0.1)w_a(\phi)\tan\phi/\gamma. \tag{3.2.1}$$

Therefore v and w are determined independently of the temperature T and Equation (2.3) for T is linear. With $s=z/\gamma$ Equation (2.3) for T becomes

$$w_a(\phi)\left[(3+s)\frac{\partial T}{\partial s}+\tan\phi\frac{\partial T}{\partial \phi}\right]=\bar{k}_a\frac{\partial^2 T}{\partial s^2}, \tag{3.2.2}$$

where $\bar{k}_a=10k/\gamma$ and the top of the abyss is at $s=-1$ with the bottom of the abyss at $s=-3$. Equations (2.1a,b,c) together with the eastern boundary condition (3.1.3) give

$$-2u\sin\phi=\gamma\left[\int_{-3}^{s}\frac{\partial T}{\partial\phi}ds'-\frac{1}{2}\int_{-3}^{-1}\int_{-3}^{s}\frac{\partial T}{\partial\phi}ds'\,ds\right]+\frac{0.2}{\gamma}(\lambda-\lambda_E)\frac{d}{d\phi}[w_a(\phi)\sin^2\phi]. \tag{3.2.3}$$

When the temperature T is determined through solving Equation (3.2.2) numerically, then u is given by (3.2.3) where the integral terms on the right hand side of (3.2.3) represent thermal wind effects and the other term represents the effect of upwelling.

From the climatological data in [10, fig. 16, p. 122] showing the annual mean potential temperature (°C) at 1500m depth, we take the temperature distribution at the top of the abyss (cf. (3.1.1)) to be given by

$$T_a(\phi)=1+1.8238\phi^2 \quad \text{when } 0\le\phi\le\pi/6,$$
$$T_a(\phi)=1.75-0.912\phi^2 \quad \text{when } \frac{\pi}{6}\le\phi\le\frac{\pi}{3}. \tag{3.2.4}$$

Note that since the reference temperature $t_0'=2.0$°C, expression (3.2.4) gives the temperature at the top of the abyss increasing quadratically from 4°C at the equator to 5°C at 30° N and then decreasing quadratically from there to 3.5°C at 60° N.

The shape of the upwelling function, $w_a(\phi)$, at the top of the abyss (cf. (3.1.1)) is chosen as follows. Since the thermocline is shallower at the equator than at 60° N, and since theoretical predictions give the upwelling velocity varying as k_z'/d, where k_z' is the coefficient of thermal diffusion and d is the thickness of the thermocline layer, this implies a larger upwelling velocity at the equator than at 60° N. We therefore take $w_a(\phi)$ to decrease linearly from the equator to 60° N, i.e. given by

$$w_a(\phi) = m\phi + c, \tag{3.2.5}$$

where m (<0) and c are parameters chosen below. The above expression (3.2.5), which gives the upwelling decreasing continuously towards the north, is consistent with results from [7], which show upwelling decreasing from the equator northwards (and also decreasing westwards from the eastern boundary).

We require that the upwelling through the surface of the abyss (i.e. the region $0 \leq \lambda \leq \lambda_E$ and $0 \leq \phi \leq \pi/3$) as given by expression (3.2.5) for $w_a(\phi)$ (scaled with upwelling velocity $W_a = 2 \times 10^{-7}$m s^{-1}) should equal the Stommel and Arons uniform upwelling given by $w_a(\phi) = 1$ in [22; 23] (also scaled with respect to W_a). This requires that

$$\int_{\lambda=0}^{\lambda=\lambda_E} \int_{\phi=0}^{\phi=\pi/3} \cos\phi \, d\phi \, d\lambda = \int_{\lambda=0}^{\lambda=\lambda_E} \int_{\phi=0}^{\phi=\pi/3} (m\phi + c)\cos\phi \, d\phi \, d\lambda, \tag{3.2.6}$$

which yields $m = 2.1283\ (1 - c)$ or $c = 1 - 0.4699m$, and gives

$$w_a(\phi) = 1 + m(\phi - 0.4699). \tag{3.2.7}$$

In [22; 23] Stommel and Arons took $m = 0$ in (3.2.7). The term on the left in Equation (3.2.6) represents the upwelling through the surface of the abyss over the total ocean region in the Stommel–Arons model, while the right-hand side of (3.2.7) represents the same quantity in the model here.

In Equation (3.2.2) for T there are now two variable parameters, i.e. m (through $w_a(\phi)$) and $\bar{k}_a$. The parabolic partial differential Equation (3.2.2) for T is solved numerically for fixed values of m and $\bar{k}_a$ (using the NAG FORTRAN Library Routine D03PAF) with boundary conditions $T = T_a(\phi)$ at $s = -1$ and $T = 0$ at $s = -3$ together with the symmetry condition $\partial T/\partial\phi = 0$ at $\phi = 0$ (the equator). Note that at $\phi = 0$ the partial differential equation reduces to an ordinary differential equation which is solved numerically to give the temperature distribution with depth at $\phi = 0$. A series of numerical experiments, by varying the values of m and $\bar{k}_a$ were performed. The relative error (R.E.) between the temperature, T (calculated here), and the climatological data (given in [10]) denoted by T_L was calculated with R.E. given by

$$\text{R.E.} = \frac{1}{n^{1/2}} \left[\left(\frac{T^1 - T_L^1}{T_L^1} \right)^2 + \ldots + \left(\frac{T^n - T_L^n}{T_L^n} \right)^2 \right]^{\frac{1}{2}}, \tag{3.2.8}$$

where $T^1, T^2, \ldots, T^n$ is the temperature at a series of latitude points $\phi_1, \phi_2, \ldots, \phi_n$ (in $0 \leq \phi \leq 60°$, with $n = 15$) and T_L^1, etc., are the equivalent values from [10] and the measurements are at a fixed depth in the abyss. R.E. was calculated at depths as follows: 2000m (i.e. $s = -1.37$) with T_L from [10, fig. 17, p. 122]; 2500m (i.e. $s = -1.74$) with T_L from [10, fig. 18, p. 123]; 3000m (i.e. $s = -2.11$) with T_L from [10, fig. 19, p. 123]; 3500m (i.e. $s = -2.48$) with T_L from [10, fig. 20, p. 123]; and a combined R.E. from the combination

TABLE 1—Values of the relative error (R.E.) for $\bar{k}_a = 1.2$ and values of m between -0.01 and -1.1 at depths of 3500m, 3000m, 2500m, 2000m and the combined depths.

m	*3500m*	*3000m*	*2500m*	*2000m*	*Combined*
−1.1	0.046	0.030	0.047	0.056	0.046
−0.9	0.043	0.025	0.039	0.051	0.041
−0.7	0.041	0.021	0.032	0.045	0.036
−0.5	0.040	0.019	0.026	0.041	0.033
−0.3	0.039	0.020	0.021	0.037	0.031
−0.1	0.039	0.023	0.018	0.033	0.030
−0.01	0.039	0.025	0.017	0.032	0.030

TABLE 2—Values of the relative error (R.E.) for $m = -0.7$ and values of $\bar{k}_a$ between 0.8 and 1.4 at depths of 3500m, 3000m, 2500m, 2000m and the combined depths.

$\bar{k}_a$	*3500m*	*3000m*	*2500m*	*2000m*	*Combined*
0.8	0.046	0.078	0.10	0.098	0.083
0.9	0.037	0.054	0.072	0.076	0.062
0.95	0.034	0.044	0.060	0.067	0.053
1.0	0.033	0.035	0.050	0.060	0.046
1.05	0.034	0.027	0.042	0.055	0.041
1.1	0.035	0.022	0.036	0.050	0.037
1.15	0.038	0.020	0.033	0.047	0.036
1.2	0.041	0.021	0.032	0.045	0.036
1.25	0.044	0.025	0.034	0.045	0.038
1.3	0.047	0.030	0.037	0.045	0.040
1.4	0.054	0.040	0.045	0.047	0.047

of these depths. Values of R.E. (as computed using (3.2.8)) are shown in Table 1 for $\bar{k}_a = 1.2$ and m varying between -0.01 (near the Stommel–Arons value in [22; 23]) and -1.1. The maximum combined R.E. (occurring at $m = -1.1$) is 0.046, or a relative percentage error of 4.6% is acceptable. This says that for all m in the range -0.01 to -1.1 a value of $\bar{k}_a = 1.2$ equivalent to $k_z' = 1.62 \times 10^{-4} \mathrm{m}^2 \mathrm{s}^{-1}$ [since $k_z' = DWk = (D\gamma)(W/10)\bar{k}_a = 1.35 \times 10^{-4} \bar{k}_a \mathrm{m}^2 \mathrm{s}^{-1}$] gives acceptably small errors between T (calculated here) and T_L. Since the primary focus of this paper is to try to identify possible variations in the magnitude of k_z' in different regions of the ocean, one value of m, i.e. $m = -0.7$ (which gives upwelling velocity at the equator of $2.66 \times 10^{-7} \mathrm{m\,s}^{-1}$), was selected, which then determines the meridional variation of upwelling from the abyss into the thermocline. This is a necessary boundary condition for the thermocline region. For $m = -0.7$, Table 2 shows R.E. (at depths: 2000m, 2500m, 3000m, 3500m, and the combined depths) for $\bar{k}_a$ in the range 0.8–1.4. It is seen that the combined R.E. is minimised by choosing $\bar{k}_a$ in the range 1.1 ($k_z' = 1.49 \times 10^{-4} \mathrm{m}^2 \mathrm{s}^{-1}$) to 1.25 ($k_z' = 1.69 \times 10^{-4} \mathrm{m}^2 \mathrm{s}^{-1}$). These values are consistent with the value for k_z' calculated in [11; 12]. Webb and Suginohara [24] suggest that a value of $k_z' = 0.3 \times 10^{-4} \mathrm{m}^2 \mathrm{s}^{-1}$ is more consistent with existing observations of mixing in the ocean. Their argument is that some of the abyssal mass rises along isothermals in the southern ocean, with the resultant need for a decrease in the diathermal upwelling over the remainder of the global ocean. This implies a smaller value for the typical abyssal upwelling velocity (W_a) than is used here with a related reduction in the typical Ekman downwelling velocity (W), since to be consistent with observations W is approximately $5W_a$ (as assumed here). Indeed if W is appropriately reduced from its value here of $10^{-6}\mathrm{m}\ \mathrm{s}^{-1}$ it is seen that values of k_z', as advocated by Webb and Suginohara in [24], do occur since $k_z' = DWk = (D\gamma)(W/10)\bar{k}_a = (1350\mathrm{m})(W/10)\bar{k}_a \mathrm{m}^2\ \mathrm{s}^{-1}$. As reported by Polzin *et al.* in [15], much larger values of k_z' (reaching $10^{-3}\mathrm{m}^2\ \mathrm{s}^{-1}$) are measured in localised regions near the rough bottom topography of the mid-Atlantic ridge. These are extreme local values for k_z', not to be compared with the averaged k_z' (averaged over the depth of the abyss) calculated here and in [11; 12; 24].

With temperature, T, now determined the zonal component of velocity, u, is given numerically through expression (3.2.3). The velocity field is then fully determined. The resulting flow field is not presented here for the following reasons. The model here is a modification of the Stommel–Arons model [22; 23] of the circulation in the abyssal ocean by allowing temperature (homogeneous in Stommel–Arons) to vary with depth and latitude. The model here (similar to Stommel–Arons) for the North Atlantic is fed from a southward-flowing western boundary current whose source is a downwelling point at the northern extremity of the basin. Some of the source fluid upwells through the top of the abyss and the remaining fluid recirculates in the abyssal region. The detailed structure of the velocity field determined here is available in Hodnett and McNamara [5], which treats the abyssal circulation in both the North Atlantic and North Pacific. The changes from the Stommel–Arons flow field are briefly as follows. The Stommel–Arons flow field is an anticyclonic gyre (fed from the western boundary current and with zonal velocity vanishing at the eastern boundary), which closes at the northern extremity source point and with uniform upwelling from the abyss into the thermocline. Here, at the ocean bottom, fluid emerging from the southward-flowing western boundary current, between $\phi = 0$ and $\phi = 30^\circ$ N approximately, flows directly into the eastern boundary from where it re-emerges, higher up the water column, to flow back to the western boundary. The fluid emerging from the western boundary current, between $\phi = 30^\circ$ N approximately and $\phi = 60^\circ$ N, recirculates in a Stommel–Arons type anticyclonic gyre except that some of this fluid also enters the eastern boundary to re-emerge higher up the water column.

Since the structure of the v, w field is so simple here we later present a schematic diagram of the v, w field which is of interest in its own right.

4. The thermocline region

For the thermocline region (between $z = 0$ and $z = -\gamma$) the boundary conditions at the bottom of the thermocline ($z = -\gamma$) are those at the top of the abyss, i.e. conditions (3.1.1) with $T_a(\phi)$ given by (3.2.4) and $w_a(\phi)$ given by (3.2.7) with $m = -0.7$.

The boundary conditions at the top of the thermocline (i.e. at depth 150m, which is the thickness of the Ekman layer) are:

$$T = T_e(\phi) \quad \text{and} \quad w = w_e(\phi) \quad \text{at } z = 0, \tag{4.1}$$

where $T_e(\phi)$ and $w_e(\phi)$ are specified as follows. From the climatological data in [10, fig. 13, p. 121] showing annual mean potential temperature (°C) at 150m depth, we take the temperature distribution at the top of the thermocline to be given by

$$\begin{aligned} T_e(\phi) &= 5 + 14.588\phi^2 \qquad \text{when } 0 \le \phi \le \pi/6 \\ T_e(\phi) &= 11.334 - 8.512\phi^2 \quad \text{when } \pi/6 \le \phi \le \pi/3. \end{aligned} \tag{4.2}$$

Note that (since the reference temperature, $t_0' = 2.0$°C), then (4.2) gives the temperature at the top of the thermocline increasing quadratically from 12°C at the equator to 20°C at 30° N and then decreasing quadratically from there to 6°C at 60° N.

The shape of the non-dimensional vertical velocity, $w_e(\phi)$, at the top of the thermocline (bottom of the Ekman layer) is chosen (following [4]) to be

$$w_e(\phi) = c[6\cos 6\phi - \sin 6\phi \tan\phi], \tag{4.3}$$

where c is a non-dimensional constant with value $c = 0.1272$. This distribution of vertical velocity results from a reasonable model of the mean wind stress (at the ocean surface) as given in [2] in representation of the observed westerlies and trade winds in the latitude range $0 \le \phi \le 60°$ N for the North Atlantic. It is noted that $w_e(\phi)$ is zero at $\phi = 14.5°$ N and $\phi = 43.5°$ N and that there is upwelling ($w_e(\phi) > 0$) through the top of the thermocline in the range $0 \le \phi < 14.5°$ N; downwelling in the range $14.5°\text{ N} < \phi < 43.5°$ N; and upwelling in the range $43.5°\text{ N} < \phi \le 60°$ N.

Applied at the eastern boundary $\lambda = \lambda_e$, is the *generalised eastern boundary condition*

$$\int_{z=-\gamma}^{z=0} u\,dz = 0 \tag{4.4}$$

4.1. Solution for the thermocline

Since T is assumed to be independent of λ then v and w are determined independently of temperature T, and in similar fashion to that described for the abyss, are derived to be

$$\begin{aligned} w &= w_e(\phi) + [w_e(\phi) - (0.2)w_a(\phi)](z/\gamma), \quad \text{and} \\ v &= [w_e(\phi) - (0.2)w_a(\phi)](\tan\phi/\gamma). \end{aligned} \tag{4.1.1}$$

Note that the solutions for w and v as given by (4.1.1) are similar in structure to w and v (in the abyss) as given by (3.2.1), and that on comparing v (in the thermocline) as given in (4.1.1) with v (in the abyss) as given in (3.2.1), there is a discontinuity in v at the thermocline/abyss interface. In contrast to these piecewise linear solutions for w in the thermocline/abyss one of the similarity solutions (considered in detail) in [18] has quadratic variation for w and hence linear variation for v over the total ocean depth.

Then Equation (2.3) for T becomes the linear equation

$$\{w_e(\phi) + [w_e(\phi) - (0.2)w_a(\phi)]s\}\frac{\partial T}{\partial s} + [w_e(\phi) - (0.2)w_a(\phi)]\tan\phi\frac{\partial T}{\partial \phi} = \bar{k}_t\frac{\partial^2 T}{\partial s^2}, \tag{4.1.2}$$

where $s = z/\gamma$ and $\bar{k}_t = k/\gamma$ and the top of the thermocline is $s = 0$ while the bottom of the thermocline is at $s = -1$. Following the same procedure as described for the abyss

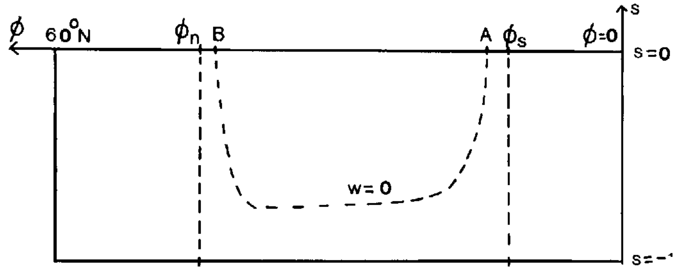

FIG. 1—Shows the thermocline region between $0 \geq s \geq -1$ and $0 \leq \phi \leq 60°$ N, where point A denotes $\phi = 14.5°$ N ($w_e(\phi) = 0$) and point B denotes $\phi = 43.5°$ N ($w_e(\phi) = 0$). In the range $0 \leq \phi < 14.5°$ N, $w_e(\phi) > 0$ (i.e. there is upwelling into the Ekman layer), while in the range $14.5°$ N $< \phi < 43.5°$ N, $w_e(\phi) < 0$ (i.e. there is downwelling from the Ekman layer) and in the range $43.5°$ N $< \phi \leq 60°$ N, $w_e(\phi) > 0$ (i.e. there is upwelling into the Ekman layer). There is no flow across the latitude lines $\phi = \phi_s \equiv 12.05°$ N and $\phi = \phi_n \equiv 45°$ N. The broken curve indicates where $w = 0$ (in the sub-tropical thermocline).

the zonal velocity component, u, is given by

$$-2u \sin\phi = \gamma \left[\int_{-1}^{s} \frac{\partial T}{\partial \phi} ds' - \int_{-1}^{0} \int_{-1}^{s} \frac{\partial T}{\partial \phi} ds' ds \right] + 2\frac{(\lambda - \lambda_E)}{\gamma} \frac{d}{d\phi} \{ [w_e(\phi) - (0.2) w_a(\phi)] \sin^2 \phi \}. \qquad (4.1.3)$$

When the temperature, T, is determined through solving Equation (4.1.2) numerically, then u is given by (4.1.3).

Note from (4.1.1) that $v = 0$ at latitudes where $w_e(\phi) = (0.2) w_a(\phi)$ (at these latitudes it is necessary that $w_e(\phi) > 0$ since $w_a(\phi) > 0$ everywhere). There are two such latitudes. One is north of $\phi = 43.5°$ N (where $w_e(\phi) = 0$) and occurs at $\phi_n = 45°$C and the other is south of $\phi = 14.5°$ N (where $w_e(\phi) = 0$) and occurs at $\phi_s = 12.05°$ N. There is no flow across the latitude lines $\phi = \phi_s$ and $\phi = \phi_n$. There are, therefore, separate solutions for the tropical thermocline ($0 \leq \phi \leq \phi_s$), the sub-tropical thermocline ($\phi_s \leq \phi \leq \phi_n$), and the sub-polar thermocline ($\phi_n \leq \phi \leq 60°$ N). However, the sub-tropical and sub-polar thermoclines are linked through the distribution, with depth of temperature at their common interface, $\phi = \phi_n$. Note also from (4.1.1) that (when $w_e(\phi) < 0$, i.e. in $14.5°$ N $\leq \phi \leq 43.5°$ N)

$$w = 0 \quad \text{when } s = -w_e(\phi)/[w_e(\phi) - (0.2) w_a(\phi)] \qquad (4.1.4)$$

for s values in the range $0 \leq s \leq -1$. Figure 1 shows a schematic of the different regions with the broken curve marking $w = 0$ (in the sub-tropical thermocline).

4.1.1. The tropical thermocline

The parabolic partial differential (4.1.2) for T is solved numerically for fixed values of $\bar{k}_t$ (as before using the NAG FORTRAN Library Routine DO3PAF) with boundary condition $T = T_e(\phi)$ (given by (4.2)) at $s = 0$, $T = T_a(\phi)$ given by (3.2.4) at $s = -1$ and with $w_e(\phi)$ and $w_a(\phi)$ specified, respectively, by (4.3) and (3.2.7), with $m = -0.7$, for ϕ in the range $0 \leq \phi \leq \phi_s = 12.05°$ N. At $\phi = 0$ the symmetry condition $\partial T / \partial \phi = 0$ is applied and also the partial differential equation (4.1.2) reduces to an ordinary differential equation that is

Table 3—Values of the relative error (R.E.) at depths of 500m and 1000m in (a) the tropical thermocline, (b) the subtropical thermocline and (c) the subpolar thermocline for a range of values of $\bar{k}_t$ between 0.025 and 1.0.

$\bar{k}_t$	0.025	0.05	0.1	0.25	0.75	1.0
Tropical						
500m	0.45	0.37	0.16	0.15	0.30	0.28
1000m	0.14	0.13	0.04	0.24	0.45	0.43
Subtropical						
500m	0.34	0.22	0.17	0.13	0.11	0.10
1000m	0.26	0.25	0.36	0.44	0.42	0.42
Subpolar						
500m	0.22	0.11	0.28	0.33	0.24	0.22
1000m	0.11	0.18	0.36	0.50	0.47	0.45

solved to yield the temperature distribution, over $-1 \leq s \leq 0$, at $\phi = 0$. The relative error (R.E. defined by (3.2.8)) between the temperature, T (calculated here) and the climatological data, T_L (given in [10]) is calculated at fixed depths 500m (i.e. $s = -0.259$) and 1000m (i.e. $s = -0.63$). T_L at 500m depth is taken from [10, fig. 14, p. 121) and T_L at 1000m depth is from [10, fig. 15, p. 122]. Values of R.E. are shown in Table 3 for a series of $\bar{k}_t$ values in the range $0.025 \leq \bar{k}_t \leq 1.0$. It is shown that in the tropical thermocline, R.E. is minimised at the combined depths of 500m and 1000m by choosing $\bar{k}_t = 0.1$ equivalent to $k_z' = 1.35 \times 10^{-4}\text{m}^2\,\text{s}^{-1}$ [since $k_z' = DWk = (D\gamma)W\bar{k}_t = 1.35 \times 10^{-3}\bar{k}_t\text{m}^2\,\text{s}^{-1}$]. The corresponding relative percentage errors of 16% at 500m and 4% at 1000m are larger than the minimised errors in the abyss, and this reflects the fact that here (in the thermocline) the parameters $w_e(\phi)$ and $w_a(\phi)$ in Equation (4.1.2) for T are specified *a priori*, but in the abyss the parameter $w_a(\phi)$ is allowed to vary (through variable values of m; cf. Table 1). The value here of $k_z' = 1.35 \times 10^{-4}\text{m}^2\,\text{s}^{-1}$, is similar in magnitude to the value of k_z' for the abyss (as calculated in Section 3.2) and consistent with the value for k_z' advocated in [11; 12]. However, if the arguments in [24] are accepted, then the value of W_a (abyssal upwelling) used here should be reduced. Since in this paper we also assumed that W (Ekman downwelling) is $5W_a$, this implies that W is also reduced. Then since $k_z' = DWk = (D\gamma)W\bar{k}_t = (1350\text{m})W\bar{k}_t\text{m}^2\,\text{s}^{-1}$, we see that if W is reduced from its value here of $10^{-6}\text{m}\,\text{s}^{-1}$ by say a factor of 5, then k_z' is reduced to $2.7 \times 10^{-5}\text{m}^2\,\text{s}^{-1}$, which is close to the value advocated by Webb and Suginohara in [24]. Alternatively, we might have reduced W_a (abyssal upwelling) and left W (Ekman downwelling) unchanged. In which case there would have been a change in structure for the equation determining temperature, T, in both the abyss and thermocline.

4.1.2. *Combined subtropical/subpolar thermocline*

To solve for the temperature, T, in either of these regions it is necessary to determine the distribution of T with depth at their common interface, $\phi = \phi_n = 45^\circ$ N, where $v = 0$ and $w = w_e(\phi_n)$. This distribution is given by the numerical solution of the ordinary differential equation, $w_e(\phi_n)(dT/ds) = \bar{k}_t(d^2T/ds^2)$, with boundary conditions. $T = T_e(\phi_n)$ at $s = 0$ and $T = T_a(\phi_n)$ at $s = -1$. With $T(\phi_n)$ so determined the partial differential Equation (4.1.2) for

T is solved for a fixed value of $\bar{k}_t$ in the subpolar thermocline by integrating northward from $\phi = \phi_n$ to $\phi = 60^\circ$ N, with the same boundary conditions as before and by the same procedure as described before. In a similar manner, the solution for T in the subtropical thermocline is determined by integrating southward (with the same value $\bar{k}_t$) from $\phi = \phi_n$ to $\phi = \phi_s = 12.05^\circ$ N. As before, R.E. at depths 500m and 1000m is calculated for each of these regions and the results are shown in Table 3 for a series of values of $\bar{k}_t$ in the range $0.025 \leq \bar{k}_t \leq 1.0$. The relative error (R.E.) can be minimised at the combined depths of 500m and 1000m by choosing (for the combined subpolar and subtropical thermocline regions) $\bar{k}_t = 0.05$, equivalent to $k_z' = 0.675 \times 10^{-4}\text{m}^2\,\text{s}^{-1}$, since $k_z' = DWk = (D\gamma)W\bar{k}_t = 1.35 \times 10^{-3}\bar{k}_t\text{m}^2\,\text{s}^{-1}$. The corresponding relative percentage errors (e.g. 25% at 1000m in the subtropical thermocline) are relatively large and can only be decreased by changing the distribution of $w_e(\phi)$, which is a significant parameter in Equation (4.1.2) for T. It is significant that the model here determines a value for k_z', in the combined subpolar/subtropical thermocline that is half its value in the tropical thermocline. This represents the major spatial variation in k_z' (as determined by the model here) since the magnitudes of k_z' in the tropical thermocline and the abyss are similar. We also note that if W is again reduced from its value here of 10^{-6}m s^{-1} by a factor of 5 (following the arguments in [24]), then k_z' is reduced to $0.135 \times 10^{-4}\text{m}^2\,\text{s}^{-1}$, which is close to the values of k_z' measured by Ledwell *et al*. [9] in the open ocean region of the subtropical thermocline (i.e. distant from the ocean side boundaries). However, the elevated values for k_z' that occur locally above the rough topography of the mid-Atlantic ridge (as measured by Polzin *et al*. [15]) also occur locally above the rough topography of the continental slope side-boundaries of the ocean. Indeed Samelson [19] considered the influence of localised regions of enhanced vertical mixing (near the ocean eastern boundary) in a numerical experiment on the stratification and circulation in a large-scale ocean model. These factors would suggest that the zonally averaged value for k_z', as determined by the model here, should lie between the open ocean value measured by Ledwell *et al*. [9] and the enhanced values observed over the ocean eastern continental slope. This average value is likely to be closer to the value determined by the model here (i.e. $k_z' = 0.675 \times 10^{-4}\text{m}^2\,\text{s}^{-1}$) than the open ocean value measured by Ledwell *et al*. [9] of $k_z' = 0.11 \times 10^{-4}\text{m}^2\,\text{s}^{-1}$.

5. Discussion

The reduced model of the ocean used here assumes that zonal variations in temperature are negligible, and makes use of a generalised eastern boundary condition requiring the integrated mass transport (over the ocean depth) rather than the zonal velocity component itself to be zero at the eastern boundary. The consequence of the zonally invariant temperature is that the velocity components v and w are independent of λ (longitude), and only the zonal velocity component, u, varies with λ and then linearly. Such a restricted model cannot, with confidence, be used to predict the magnitude for k_z' (vertical thermal diffusion coefficient) in a large-scale ocean. However, the primary focus of the paper was to identify possible spatial variations in the magnitude of k_z' (consistent within the model) in different regions of the ocean. In this sense the significant result from the model is that the value of k_z' in the combined subpolar/subtropical thermocline is half its value in the tropical thermocline and approximately 40% of its value in the abyssal region. It transpires that the resultant ocean average value for k_z' is near the value of $10^{-4}\text{m}^2\,\text{s}^{-1}$ as calculated in

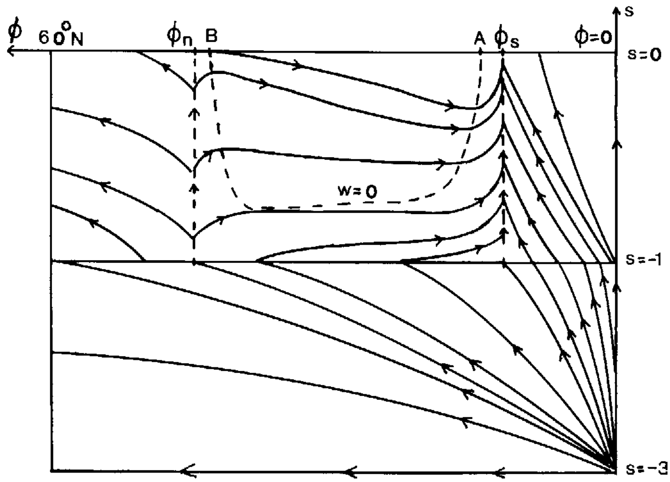

FIG. 2—A schematic representation of the v, w flow field in the thermocline ($0 \geq s \geq -1$) and abyss ($-1 \geq s \geq -3$). The relative depths of the thermocline and abyss are not drawn to scale. The broken curve shown in the subtropical thermocline is where $w = 0$. Points A, B, ϕ_n, ϕ_s are as defined in Figure 1. There is no flow (in the thermocline) across the latitude lines $\phi = \phi_s \equiv 12.05°$ N and $\phi = \phi_n \equiv 45°$ N. Note that v is discontinuous at $s = -1$ (in fact v reverses sign there when ϕ is in the range $\phi_s < \phi < \phi_n$).

[11; 12]. This is a consequence of assuming (following [22; 23] and others) that the abyssal upwelling velocity, $W_a = 2 \times 10^{-7}$m s^{-1} and (to be consistent with observations) that the Ekman downwelling velocity, $W = 10^{-6}$m s^{-1}. In [24], Webb and Suginohara suggest that W_a (and hence W based on the assumption made in this paper) should be reduced, and if both W_a and W are reduced by a factor of 5 then the average value for k_z^I is close to the value of 3×10^{-5}m^2 s^{-1} as advocated by Webb and Suginohara in [24].

It is instructive to plot the (v, w) element of the flow field from expression (3.2.1) for v and w in the abyss and expression (4.1.1) for v and w in the thermocline, and this is done schematically in Fig. 2, where the broken curve (in the subtropical thermocline) represents $w = 0$. It is interesting to note that the variation with depth of w (vertical velocity) in the subtropical region, where the magnitude of the downward vertical velocity decreases linearly from its surface value to zero (at the curve $w = 0$) and from there increases linearly to a maximum upward vertical velocity at the top of the abyss from where it decreases linearly to zero at the bottom of the abyss, is similar to that reported by Samelson and Vallis [20] in the centre of their subtropical gyre. In their paper Samelson and Vallis considered large-scale circulation with small vertical thermal diffusion (i.e. $k_z^I = 0.1 - 0.5 \times 10^{-4}$m^2 s^{-1}) and identified, in the subtropical region (i.e. region of Ekman downwelling), two thermocline regions with an upper advectively-dominated region above a lower diffusively-dominated region. The significance of these similarities in the structure for w (here and in [20]), lies in the fact that when w varies linearly with depth (as here) then v is independent of depth and this structure for the v, w field is a result of the assumption that $\partial T/\partial \lambda$ is zero, although Samelson and Vallis [20] make no such global assumption with respect to the distribution of T.

ACKNOWLEDGEMENT

The authors are grateful to John Huthnance and Roger Samelson for helpful comments on a draft of this paper.

REFERENCES

[1] C.A. Edwards and J. Pedlosky, The influence of distributed sources and upwelling on the baroclinic structure of the abyssal circulation, *Journal of Physical Oceanography* **25** (1995), 2259–84.

[2] A.J. Evenson and G. Veronis, Continuous representation of wind stress and wind stress curl over the world ocean, *Journal of Marine Research* (*Suppl.*) (1975), 131–44.

[3] A.E. Gill, An explicit solution of the linear thermocline equations, *Tellus* **37**A (1985), 276–85.

[4] P.F. Hodnett and A.R. Ansari, Interaction of a simple ocean model with various eastern boundary shapes, *Geophysical and Astrophysical Fluid Dynamics* **78** (1994), 73–93.

[5] P.F. Hodnett and R. McNamara, A modified Stommel–Arons model of the abyssal ocean circulation, *Mathematical Proceedings of the Royal Irish Academy* **100**A (1) (2000), 85–104.

[6] R.X. Huang, The generalised eastern boundary conditions and the three-dimensional structure of the ideal fluid thermocline, *Journal of Geophysical Research* **94** (1989), 4855–65.

[7] R.X. Huang, A two-level model for the wind and buoyancy forced circulation, *Journal of Physical Oceanography* **23** (1993), 104–15.

[8] G.S. Janowitz, A surface density and wind driven model of the thermocline, *Journal of Geophysical Research* **91** (1986), 5111–18.

[9] J.R. Ledwell, A.J. Watson and C.S. Law, Mixing of a tracer in the pycnocline, *Journal of Geophysical Research—Oceans* **103** (1998), 21499–529.

[10] S. Levitus, *Climatologial atlas of the world ocean*, NOAA Technical paper 13, National Oceanic and Atmospheric Administration, Rockville, Maryland, 1982.

[11] W.H. Munk, Abyssal recipes, *Deep-Sea Reseach*, **13** (1966), 707–30.

[12] W.H. Munk and C. Wunsch, Abyssal recipes II: energetics of tidal and wind mixing, *Deep-Sea Research* **45** (1998), 1977–2010.

[13] J. Pedlosky, Eastern boundary ventilation and the structure of the thermocline, *Journal of Physical Oceanography* **13** (1983), 2038–44.

[14] J. Pedlosky, The baroclinic structure of the abyssal ocean circulation, *Journal of Physical Oceanography* **22** (1992), 652–9.

[15] K.L. Polzin, J.M. Toole, J.R. Ledwell, *et al*., Spatial variability of turbulent mixing in the abyssal ocean, *Science* **276** (1997), 93–6.

[16] R. Salmon, A simplified linear ocean circulation theory, *Journal of Marine Research* **44** (1986), 695–711.

[17] R. Salmon, The thermocline as an 'internal boundary layer', *Journal of Marine Research* **48** (1990), 437–69.

[18] R. Salmon and R. Hollerbach, Similarity solutions of the thermocline equations, *Journal of Marine Research* **49** (1991), 249–80.

[19] R.M. Samelson, Large-scale circulation with locally enhanced vertical mixing, *Journal of Physical Oceanography* **28** (1998), 712–26.

[20] R.M. Samelson and G.K. Vallis, Large-scale circulation with small diapycnal diffusion: the two-thermocline limit, *Journal of Marine Research* **55** (1997), 223–75.

[21] H. Stommel, The abyssal circulation, *Deep-Sea Research* **5** (1958), 80–82.

[22] H. Stommel and A.B. Arons, On the abyssal circulation of the world ocean, I. Stationary planetary flow patterns on a sphere, *Deep-Sea Research* **6** (1960), 104–54.

[23] H. Stommel and A.B. Arons, On the abyssal circulation of the world ocean, II. An idealised model of the circulation pattern and amplitude in ocean basins, *Deep-Sea Research* **6** (1960), 217–33.

[24] D.J. Webb and N. Suginohara, The interior circulation of the ocean, in G. Siedler, J. Church and J. Gould (eds), *Ocean circulation and climate*, Academic Press, pp 205–13.

[25] P. Welander, A zonally uniform regime in the oceanic circulation, *Journal of Physical Oceanography*. **6** (1976), 121–4.

[26] Y. Yuan, P.F. Hodnett and J.M. Huthnance, Simulated influence of an eastern boundary slope current on a zonally uniform ocean model, *OMEX-1 Final Report CD-Rom*, Brussels, 1996.